Exchange Mechanisms in Europium Chalcogenides

Abstract: Superexchange mechanisms, which are mostly responsible for the nnn exchange constant I_2 in Eu chalcogenides, are investigated in detail. In contrast with the usual 3d transition metal compounds, the Kramers-Anderson mechanism is estimated to be one order of magnitude too small to explain the experimental results due to a small $4f \rightarrow 2p$ transfer energy. The mechanism by which a p electron is transferred to a 5d state through the d-f exchange interaction gives the correct order of magnitude for I_2 , with a negative sign, even though it is a sixth-order perturbation. The cross term between the above two mechanisms is shown to be nearly as important as the second mechanism and may have a positive sign. The indirect exchange mechanisms, in which the anion p level has no important role, are responsible for the nn exchange constant I_1 . The phonon-assisted mechanism proposed by Smit is estimated to be more than one order of magnitude smaller than the experimental value. The d-f mixing term is proved to be responsible for I_1 , in good agreement with experiment.

Introduction

The mechanism of exchange interaction between two localized spins at the lattice points \mathbf{R}_n and \mathbf{R}_m was first investigated by Heisenberg¹ and led to the famous Heisenberg type exchange interaction,

$$-2I_{nm}\mathbf{S}_{n}\cdot\mathbf{S}_{m},\tag{1}$$

in which the exchange constant I_{nm} is expected to originate from the overlap of two atomic orbitals centered on different sites, because of the exchange integral due to the Coulomb interaction between them. This is called the direct exchange interaction, and was initially considered to be the origin of ferromagnetism in the iron series. However, it is recognized now that the exchange mechanism in the iron series is much more complicated.¹

Later Zener² considered a mechanism in which the 3d spins are aligned through the exchange interaction with the conduction electrons of dominantly 4s character. This is called the s-d exchange mechanism and is classified as an indirect exchange mechanism. Since Zener treated only the diagonal term, his s-d exchange mechanism causes only ferromagnetic alignment. An improved treatment, given by Kasuya,³ includes nondiagonal terms and therefore the s-d scattering term. It has been shown that this mechanism causes both ferro- and antiferromagnetic alignment. The materials in which this mechanism should be applicable are rare earth metals and alloys, because of the localized character of the 4f state; various magnetic properties of these materials have been well explained by the s-f exchange model with further refinements.⁴

Another kind of indirect exchange mechanism has been developed by Kramers and Anderson⁵ for non-metallic 3d compounds. In this mechanism, the virtual transfer of a 3d electron from one site to another through the p states of the bridging anion is important and is called the superexchange mechanism. This mechanism has been investigated theoretically in detail for 3d compounds, with good qualitative agreement with experiments.^{5,6} A quantitative first-principles estimate is more complicated than expected due to various correlation, or many-body, effects.⁷

The exchange mechanisms in non-metallic rare earth compounds have not yet been studied in detail, one reason being that the interaction is usually very small due to the well-shielded character of the 4f state. In some compounds, however, the Curie temperature T_c is relatively high, for example 70°K in EuO. The exchange mechanisms in rare earth compounds may be different from those in 3d compounds in the following ways: First, 4f electrons are well shielded by the 5s and 5p closed shells, and the ionic radius is determined by these closed shells. Thus the polarization effects of these 5s and 5p shells may be important. This was particularly emphasized by Watson and Freeman,⁸ who discussed the crystal field effects due both to the static lattice potential and to the covalent bonding effect. The experimental evidence is not clear, however. Second, the conduction bands are now constructed from both 6s and 5d states. The overlapping between 5d states is sufficiently large to form a good conduction band because the 5d wave functions are more extended than those of the 5s and 5p electrons. This makes possible a new indirect mechanism through the 5d bands. Third, as mentioned before, the 4f state is well inside the ionic radius,

The author is located at the IBM Thomas J. Watson Research Center, Yorktown Heights, New York 10598.

while the ionic radius of a 3d element is determined by the radius of the 3d state itself. This makes the localized view of the magnetic electrons very sound, and also may change the relative importance of various competing mechanisms. Fourth, some convenient dilute alloys may have a very small number of free or loosely bound conduction electrons. Thus the s-f or d-f exchange mechanism in such materials will have different features from that in good metals. Detailed treatment may cast a new light on the character of the s-f exchange mechanism. It is also expected that new information obtained for rare earth compounds will make possible the reinterpretation of exchange mechanisms in the 3d compounds.

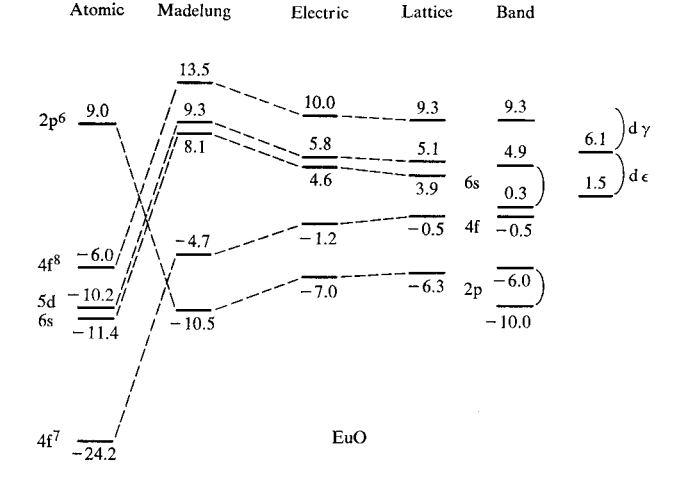
In the following sections polarization effects of 5s and 5p electrons will be neglected for simplicity. This means that the effects may be included as the "effective" 4f radius. The more detailed effects of shielding have not as yet been established experimentally.

A large body of experimental results has been accumulated on the Eu chalcogenides and their alloys. ¹⁰ This is a simple system with the rock salt type of structure and the simple magnetic configuration ⁸S. Therefore our calculations are done for these materials and compared with experiment.

In the following, the exchange mechanisms are classified among the following categories: superexchange, indirect exchange, s-f exchange and higher-order exchange. The last two are not treated in this paper.

Summary of Eu chalcogenides

In this section, a summary of the experimental data and their interpretation is given. In Fig. 1 the one-electron energy spectra of EuSe and EuO are given. These are calculated from atomic spectra data and the pure ionic crystal model, including the Madelung potential $E_{\rm M}$ and the polarization energy. 11 The energy level for a filled state is the ionization energy and that for a vacant state is the affinity energy. Figure 2 is the expected band scheme based on Fig. 1 in which the 4f level is the lowest atomic ionization energy for the ⁸S(4f⁷) configuration or, in other words, a small magnetoelectric polaron state of a 4f⁷ hole. This is consistent with the scheme proposed by Yanase and Kasuya¹² but very much different from those of Cho¹³ and Busch et al. 14 The conduction band is similar to that of Ni but with a smaller s-d mixing effect because here the 5d and 6s states are more localized than are the 3d and 4s states in the metal. 15 In Fig. 3 the values of the nn and the nnn exchange constants, I_1 and I_2 respectively, are plotted as functions of R_0 , the anion-cation distance. The idea of McGuire et al. 16 to plot I_1 as a function of the anion-cation distance is interesting and very important, as will be discussed later. Note that no data are available for the I_2 of EuO because it is much smaller than I_1 , but that the extrapolation from EuTe to EuS shows that



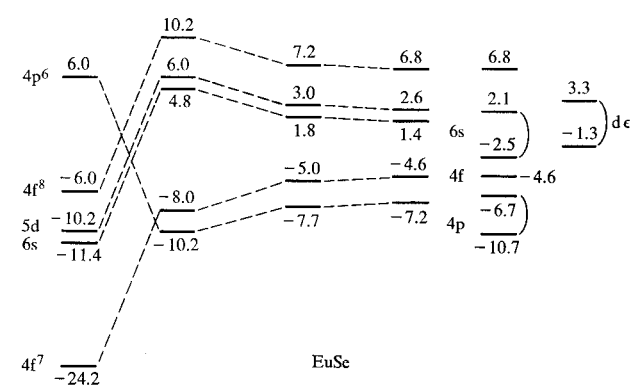


Figure 1 Energy level diagrams for EuO and EuSe; the energy units are eV. For Eu and O respectively, the Madelung potentials are \pm 19.5 eV, the electric polarization energies are both 3.5 eV, and the lattice polarization energies are both 0.7 eV. For Eu and Se respectively, the Madelung potentials are \pm 16.2 eV, the electric polarization energies are 3.0 and 2.5 eV, and the lattice polarization energies are 0.4 and 0.5 eV.

the I_2 of EuO may be of positive sign with a value of about 5×10^{-6} eV. For EuTe the value of I_1 is not well defined because it is much smaller than I_2 . From the extrapolation, it is nearly zero. In Fig. 4 various atomic wave functions are shown. Tables 1, 2 and 3 summarize some of the Eu chalcogenide data used in the text and figures.

Superexchange mechanisms (I₂)

In this category the indirect exchange mechanisms, in which the p states of an anion play important roles in the intermediate excited states, are included. Here we consider three mechanisms, the usual Kramers-Anderson mechanism, a new mechanism in which an anion p electron is transferred to a 5d state through the d-f exchange interaction, and the cross term between these mechanisms. The third term is particularly interesting because it may give the ferromagnetic superexchange interaction constant for the 180-degree configuration.

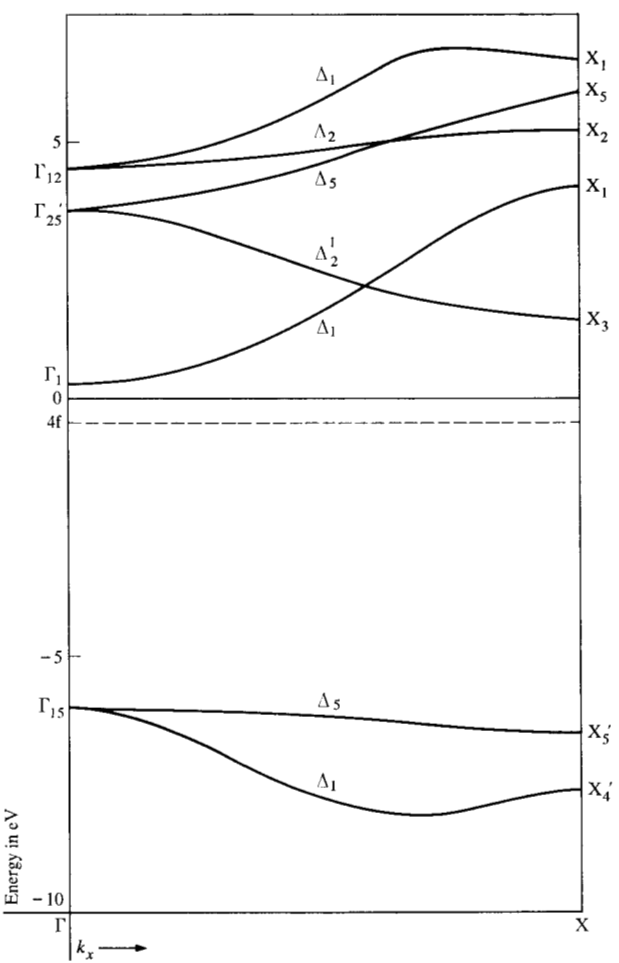


Figure 2 Schematic band structure of EuO based on Fig. 1. The dashed line is the lowest ionization energy of the ⁸S(4f⁷) configuration.

For the rock salt structure the p_{σ} anion wave function connects the two nn cations, which are nnn to each other, in the 180-degree configuration. Therefore the superexchange mechanisms provide the principal contributions to I_2 .

• Kramers-Anderson (KA) mechanism

This is a well-known mechanism, and for the rock-salt-type structure the most important contribution is due to the 180-degree configuration. The Kramers-Anderson mechanism is a fourth-order term, or, if the effective $4f_{\nu} \rightarrow 4f_{\mu}$ transfer energy $t(f_{\nu}, f_{\mu})$ is used, it is a second-order term. The exchange integral is given by

$$I_2^{(KA)} = -\frac{1}{2S^2} \sum_{\nu,\mu} \frac{|t(f_{\nu}, f_{\mu})|^2}{U(f, f)},$$
 (2)

where U(f, f) is the average energy necessary to transfer

Table 1 Europium chalcogenide data.*

	$R_0(\mathring{A})$	$E_{\rm M}(eV)$	ϵ_{∞}	ϵ_0	$\omega_{\rm to}(cm^{-1})$	$\omega_{1o}(cm^{-1})$
EuO	2.57	19.5	5.3	25.0	199	420
EuS	2.98	16.8	5.0	11.0	178	280
EuSe EuTe	3.10 3.30	16.2 15.2	4.8	9.5	128	180

* The optical and static dielectric constants are ε_{∞} and ε_{0} , respectively; ω_{10} is the Reststrahlen frequency and $\omega_{10} = \omega_{10}(\varepsilon_{0}/\varepsilon_{\infty})^{1/2}$ is the frequency of the lowest longitudinal optical mode. These data are due to J. D. Axe, J. Phys. Chem. Solids 30, 1403 (1969).

Table 2 Relative energy levels in (eV).*

	<i>U</i> (p, f)	<i>U</i> (p, d)	U(f, f)	<i>U</i> (f, d)	<i>U</i> (f, p)
EuO	17.0	12.8	11.2	7.0	5.8
EuSe	14.9	10.7	12.2	8.0	2.7

* The data are energy differences derived from the electric polarization energy column of Fig. 1; U(1, 1') denotes the difference in energy between occupied level 1 and unoccupied level 1'. However, both levels are occupied in the case of U(f, p).

Table 3 Atomic-exchange and spin-orbit constants (in cm⁻¹).*

	$I_{s\mathrm{f}}$	$I_{ m pf}$	$I_{ m df}$	λ_p	λ_{d}
Eu ⁺	209	114	787	1610	648
Gd ⁺⁺	294	246	1013	3050	1050

^{*} These data are from Table 3 of T. Kasuya and A. Yanase, Rev. Mod. Phys. 40, 684 (1964).

a 4f electron onto a 4f state of a nnn site and produce a pair of ions, Eu⁺⁺⁺ and Eu⁺. The transfer energy is given by

$$t(f_{\nu}, f_{\mu}) = -\sum_{i} t(p_{i}, f_{\nu})t(f_{\mu}, p_{i})/U(p_{i}, f), \qquad (3)$$

in which $U(p_i, f_r)$ is the energy necessary to transfer a p_i electron from an anion onto a $4f_r$ state of the nn cation and $t(p_i, f_r)$ and $t(f_r, p_i)$ are the transfer energies for $p_i \rightarrow f_r(4f^8)$ and $f(4f^7) \rightarrow p_i$, respectively. For a more detailed treatment, the final $4f^6$ and $4f^8$ configurations should be defined in the given crystal environment. In that case the anisotropic exchange interaction, or in general the anisotropy term, is obtained. Here such terms are omitted, based on the assumption that the energy differences within the important $4f^6$ and $4f^8$ multiplets are much smaller than U.

An estimate of $I_2^{(KA)}$ is made from Eq. (2) for a Eu chalcogenide as follows. The values for U are obtained from Table 2. We use the $p \rightarrow f$ and $f \rightarrow p$ transfer energies only for p_{σ} . There are several ways to estimate the transfer energy. First, the transfer energy $t(p_{\sigma}, f_{\sigma})$ in EuF₂ has been estimated by Axe and Burns¹⁷ using the Wolfberg-Helmholtz method and also by Watson and Freeman¹⁸ from a more fundamental standpoint. The expected value is about 0.4 eV. Note that the 2p wave functions, and therefore the ionic radii, of F and O are very similar and thus the nn Eu-F and Eu-O distances are also nearly equal. Therefore the above value may be applicable for the case of EuO. Second, in Cho's band calculation¹³ for EuS, the 4f levels are treated as if they lead to the usual simple bands. The overall bandwidth is estimated to be about 0.3 eV for the unoccupied 4f levels. This should correspond in the present picture approximately to

$$4t'(\mathbf{f}_{\sigma}, \mathbf{f}_{\sigma}) = 4|t(\mathbf{p}_{\sigma}, \mathbf{f}_{\sigma})|^{2}/U(\mathbf{p}, \mathbf{f})$$
(4)

and, since U(p, f) is about 2.8 eV in Cho's band calculation, we get $|t(p_{\sigma}, f_{\sigma})| = 0.46$ eV for EuS. Note that in the present energy scheme the simple $4f^7$ hole bandwidth for perfect ferromagnetic alignment is given by

$$4|t(\mathbf{f}_{\sigma}, \mathbf{p}_{\sigma})|^{2}/U(\mathbf{f}, \mathbf{p}) \tag{5}$$

and, using $t(f_{\sigma}, p_{\sigma}) = 0.4 \text{ eV}$ and U(f, p) = 5.8 eV, which is the energy difference between the 2p and $4f^7$ levels for EuO, we get a value for (5) of 0.11 eV. Third, the overall crystal field splitting of a 4f state in Eu⁺⁺⁺ (4f⁶) due to the antibonding effect with the anion is given by

$$2|t(\mathbf{f}_{\sigma}, \mathbf{p}_{\sigma})|^{2}/U(\mathbf{f}, \mathbf{p}) \tag{6}$$

or, for small values of U(f, p), by

$$\frac{1}{2}\{[|U(f, p)|^2 + 8|t(f_{\sigma}, p_{\sigma})|^2]^{\frac{1}{2}} - U(f, p)]\}. \tag{6'}$$

This value is 0.05 eV in EuO and 0.11 eV in EuSe, for $t(f_{\sigma}, p_{\sigma}) = 0.4$ eV and the values listed in Table 1. There are no data available for the crystal field splitting of 4f levels in Eu chalcogenides. However, judging from various experiments in other rare earth compounds, ¹⁹ we think these values are reasonable. Therefore the transfer energy is also very likely to be about 0.4 to 0.5 eV. Using these values we have for Eu chalcogenides

$$|t(p_{\sigma}, f_{\sigma})| \approx |t(f_{\sigma}, p_{\sigma})| \approx 0.45 \text{ eV}.$$
 (7)

Then we get, using Table 2,

$$I_2^{(KA)} = \begin{cases} 0.5 \times 10^{-6} \text{ eV} & \text{for EuO;} \\ 0.6 \times 10^{-6} \text{ eV} & \text{for EuSe.} \end{cases}$$
 (8)

For EuSe this exchange integral is about 1/20 of the experimental value. We expect some ambiguity in determinations of the transfer energy, but it cannot be large enough to cover this discrepancy.

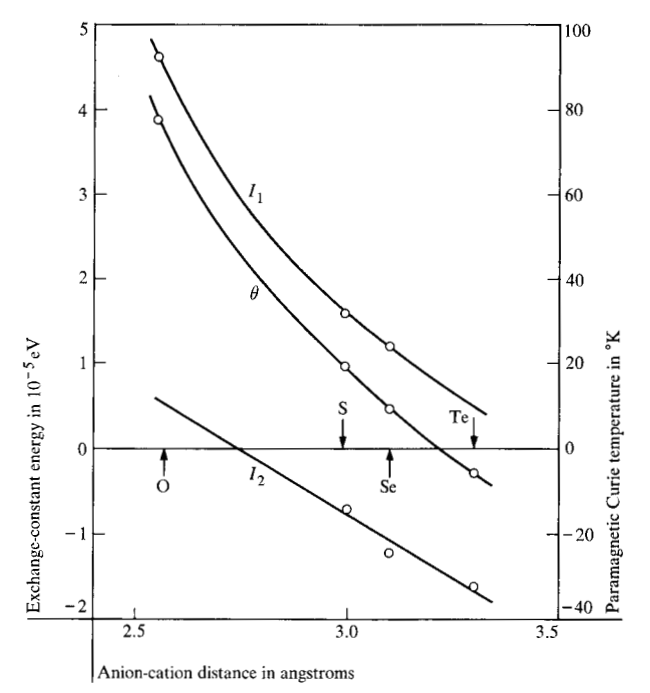
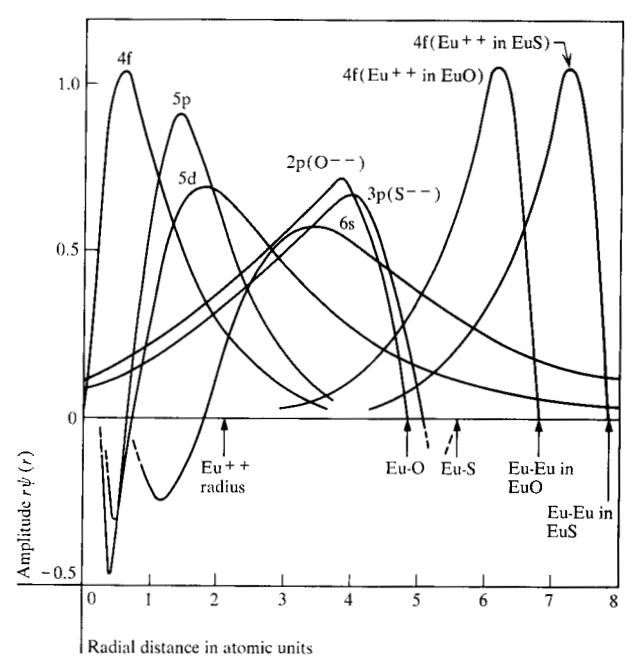


Figure 3 The exchange constants I_1 and I_2 and the paramagnetic Curie temperature θ of Eu chalcogenides as functions of the anion-cation separation R_0 . Experimental data are denoted by o's and the solid lines are extrapolated curves.

Figure 4 Atomic wave functions for Eu⁺⁺, O⁻⁻ and S⁻⁻. Lattice distances between nearest neighbor Eu and chalcogen ions are indicated by arrows, and four of the wave functions are drawn with the respective origins at these points to show the overlap of anion-cation and cation-cation functions.



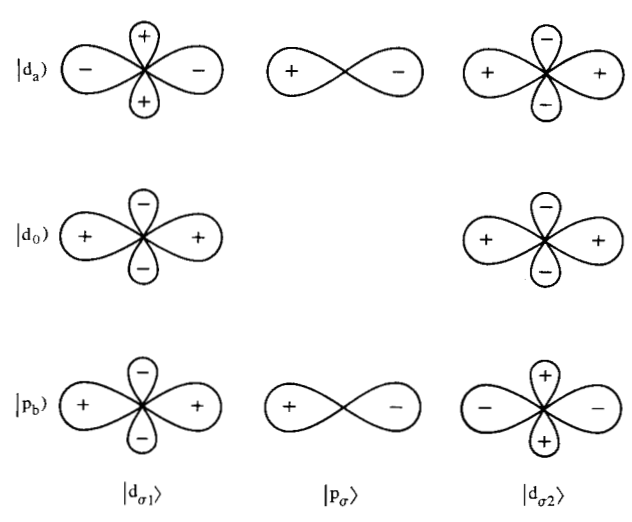


Figure 5 Composition of the molecular orbitals from the atomic orbitals.

• Superexchange via the d-f exchange interaction

The Kramers-Anderson mechanism gives too small a value for I_2 because of the small effective transfer energy $t(f_\sigma, f_\sigma)$ and this is due to the small overlap between the 2p and 4f states, which is estimated to be about 0.018 for ${}^8\mathrm{S}(p_\sigma, f_\sigma)$ in $\mathrm{Eu}F_2$. Then the following mechanism, in which the anion p electron is transferred to the 5d or 6s state of the nn Eu cation and aligns the 4f spins through the d-f or s-f exchange interaction, should be important due to a large overlap between 2p and 5d or 6s states. As the d-f exchange is usually much larger than the s-f exchange, the 5d states seem to be the more important states in Eu chalcogenides. Therefore, in the following we treat (as a typical example) only the 5d states. There are no differences at all for the 6s case or for the s-d mixed-band case.

The most important process in this mechanism is as follows. We consider the three atomic wave functions $|\mathbf{d}_{\sigma 1}\rangle$, $|\mathbf{d}_{\sigma 2}\rangle$ and $|\mathbf{p}_{\sigma}\rangle$ and determine the eigenstates, taking into account the transfer energy $t(\mathbf{p}_{\sigma}, \mathbf{d}_{\sigma})$ between them. Then the molecular orbitals $|\mathbf{d}_{0}\rangle$, $|\mathbf{d}_{a}\rangle$ and $|\mathbf{p}_{b}\rangle$, as illustrated in Fig. 5, are given by

$$|\mathbf{d}_0\rangle \equiv |\mathbf{d}_+\rangle,\tag{9a}$$

$$|\mathbf{d}_{a}\rangle = \alpha_{a}|\mathbf{p}_{\sigma}\rangle + \beta_{a}|\mathbf{d}_{-}\rangle$$
 (9b)

and

$$|\mathbf{p}_{b}\rangle = \alpha_{b}|\mathbf{p}_{\sigma}\rangle + \beta_{b}|\mathbf{d}_{-}\rangle,$$
 (9c)

in which

$$|\mathbf{d}_{\pm}\rangle \equiv \frac{1}{2}(|\mathbf{d}_{\sigma 1}\rangle \pm |\mathbf{d}_{\sigma 2}\rangle) \tag{10}$$

and α and β are approximately given by

$$\alpha_{\rm a} = -\beta_{\rm b} = 2^{\frac{1}{2}} t(p_{\sigma}, d_{\sigma}) / U(p, d) \tag{11}$$

218 and

$$\alpha_{\rm b} = \beta_{\rm a} = (1 - \beta_{\rm b}^2)^{\frac{1}{2}}. \tag{12}$$

The bonding or antibonding energy is

$$\Delta E = \pm 2|t(p_{\sigma}, d_{\sigma})|^2/U(p, d). \tag{13}$$

The transition matrix elements of these states due to the d-f intra-atomic exchange interaction are given by

$$\langle \mathbf{p}_{b} | H_{df} | \mathbf{d}_{a} \rangle = \frac{1}{2} \beta_{a} \beta_{b} I_{df} \mathbf{d}_{d} \cdot (\mathbf{S}_{f1} + \mathbf{S}_{f2}) \tag{14a}$$

and

$$\langle p_b | H_{df} | d_0 \rangle = -\frac{1}{2} \beta_b I_{df} \delta_d \cdot (S_{f1} - S_{f2}),$$
 (14b)

in which σ_d is the Pauli spin operator for the d_σ state. The second-order perturbation energy can be calculated and we are interested in the cross term because the coefficient of this term gives the exchange integral. Thus

$$I_{2}^{(\mathrm{df})} = \frac{1}{4}\beta_{\mathrm{b}}^{2} |I_{\mathrm{df}}|^{2} \left[\frac{\beta_{\mathrm{a}}^{2}}{E(\mathrm{d}_{\mathrm{a}}) - E(\mathrm{p}_{\mathrm{b}})} - \frac{1}{E(\mathrm{d}_{0}) - E(\mathrm{p}_{\mathrm{b}})} \right]$$
(15)

or, using the same approximation as in Eqs. (11) to (13),

$$I_2^{(\mathrm{df})} = -\frac{1}{2} |\beta_{\rm b}|^4 |I_{\rm df}|^2 / |U(p, d)|^5$$
 (16)

It is clear that this calculation always gives antiferromagnetic coupling. In contrast with the usual superexchange mechanism, given by Eq. (2), this mechanism is higher order, in fact sixth order, with respect to U. The expression contains an extra factor due to the d-f exchange interaction, $|I_{\rm df}S_{\rm f}/U({\rm p,d})|^2$. However, when the ${\rm p_\sigma - d_\sigma}$ transfer energy is much larger than that of ${\rm p_\sigma - f_\sigma}$, the ratio of these energies may overcome the above factor and then the present mechanism is dominant. This is actually the case in Eu chalcogenides, as shown below.

For the calculation, $t(p_{\sigma}, d_{\sigma})$ or β_b should be determined. The transfer energy between p_{σ} and d_{σ} has been estimated in various 3d transition metal compounds.²¹ The most reliable value seems to be obtained from the crystal field splitting data. In most 3d compounds with a cubic environment, the crystal field splitting, 10Dq, seems to be determined mostly by covalency effects between 3d and 2p states. Therefore, we assume here that the optically observed splitting is due to covalency. Again we neglect everything other than the p_{σ} - d_{σ} overlap²²; this causes an underestimation of $t(p_{\sigma}, d_{\sigma})$. Then

$$10Dq = 2|t(p_{\sigma}, d_{\sigma})|^{2}/U(p, d) = \beta_{b}^{2}U(p, d).$$
 (17)

Now, taking the values 10.7 eV for U(p, d) and 2 eV for 10Dq of EuSe, 23 we get

$$\beta_{\rm b}^{\ 2} = 0.187,\tag{18}$$

$$|t(p_{\sigma}, d_{\sigma})| = 3.27 \text{ eV}.$$
 (19)

This value of the transfer energy can be compared with Cho's band calculation. The bonding effect between p_{σ} and 6s or d_{σ} appears in the band calculation as the humps of the Δ_1 curves. This is seen on the highest- and the lowest-energy curves in Fig. 2. In Cho's band structure, this hump is estimated to be about 1.5 eV. Assuming t to be the p_{σ} - d_{σ} transfer energy, we get $4t^2/U = 1.5$ eV. Putting U = 13 eV for Cho's band structure, we get $t(p_{\sigma}, d_{\sigma}) = 2.2$ eV, slightly smaller than the value (19).

Now, using Eq. (18) and $I_{df} = 0.1$ eV, we get

$$I_2^{(\text{df})} = -1.6 \times 10^{-5} \text{ eV for EuSe.}$$
 (20)

The agreement with the experimental value, -1.2×10^{-5} eV, is very good. It seems clear, therefore, that d-f exchange is the main mechanism of I_2 in EuS, EuSe and EuTe. However, the decrease of I_2 with decreasing lattice constant is rather sharp, and I_2 of EuO seems to be positive. This behavior appears to indicate a competing mechanism that causes ferromagnetic coupling in the 180-degree configuration.

• Cross term

The cross term between the Kramers-Anderson and the d-f exchange mechanisms must be checked carefully because it may overcome both mechanisms and may have a different sign.

The same 180-degree configuration is considered; the molecular orbitals are constructed from $|d_{\sigma 1}\rangle$ and $|p_{\sigma}\rangle$ as follows:

$$|\mathbf{p}_{b}\rangle = \alpha_{b}^{1}|\mathbf{p}_{\sigma}\rangle + \beta_{b}^{1}|\mathbf{d}_{\sigma 1}\rangle \tag{21a}$$

and

$$|\mathbf{d}_{\mathbf{a}}\rangle = \alpha_{\mathbf{a}}^{-1}|\mathbf{p}_{\sigma}\rangle + \beta_{\mathbf{a}}^{-1}|\mathbf{d}_{\sigma 1}\rangle, \tag{21b}$$

with

$$\beta_{\rm b}^{\ 1} = -t(p_{\sigma}, d_{\sigma})/U(p, d) = -\alpha_{\rm s}^{\ 1}.$$
 (22)

The matrix element due to the d-f exchange interaction at site 1 is

$$(p_b|H_{df}(1)|d_a) = -\beta_a^{-1}\beta_b^{-1}I_{df}\delta_d \cdot S_{f1}.$$
 (23)

The third-order cross-perturbation, in which the processes $|p_b\rangle \to |d_a\rangle$, $|4f_2\rangle \to |p_b\rangle$ and $|d_a\rangle \to |4f_2\rangle$ occur in this sequence or the reversed sequence, is responsible for the exchange interaction between S_{f1} and S_{f2} and gives the coupling constant

$$I_{2}^{(e)} = 2\alpha_{a}^{1}\alpha_{b}^{1}\beta_{a}^{1}\beta_{b}^{1}I_{df} |t(p_{\sigma}, f_{\sigma})|^{2}/[S_{f}U(p, d)U(f, d)]$$

$$= -2I_{df} |t(p_{\sigma}, d_{\sigma})|^{2}$$

$$\times |t(p_{\sigma}, f_{\sigma})|^{2}/[S_{f} |U(p, d)|^{3} |U(f, d)]. \tag{24}$$

This expression is, as expected, fifth order with respect to U. The important character of this mechanism is that

its sign is opposite to that of I_{df} , or I_{sf} . For a well-localized state in a crystal, the magnitude of $I_{\rm df}$ or $I_{\rm sf}$ should be similar to the atomic value listed in Table 3. This is the case for $I_{\mathrm{df}},$ where the d ϵ or Γ_{25} states are concerned, because they do not mix with the p states and the mutual overlap is not as large as that for the transition metals. The experiments¹² seem to support this argument which, with lesser accuracy, is applicable also to $I_{\rm sf}$ in Eu chalcogenides for electrons near the bottom of the 6s band.²⁵ For d_{σ} , which is related to $d\gamma$, or Γ_{12} , the situation is very different because the overlap with the anion p state is very large. In this case the interatomic exchange due to the overlap with p_{σ} states is more important. This kind of interatomic exchange is mostly due to the nonorthogonality²⁶ of the overlapping states and has a negative sign,²⁷ opposite to that of the intra-atomic Coulomb exchange interaction. This is the usual case for the 3d transition metals, in which the sign of the s-d exchange interaction is negative, as is clear from the observation of the Kondo anomaly.²⁸ A rough estimate of the effect of interatomic exchange in Eu chalcogenides is given by a secondorder perturbation calculation of the $p_{\sigma} \rightarrow f_{\sigma}$ transfer

$$I_{\rm df}^{\rm inter} = 16|\beta_{\rm b}|^2 |t(p_{\sigma}, f_{\sigma})|^2 / U(d_{\sigma}, f_{\sigma}). \tag{25}$$

Using the values estimated for β_b and $t(p_\sigma, f_\sigma)$ and 2 eV for $U(d_\sigma, f_\sigma)$ of EuO from the last column of Fig. 1, we get $I_{\rm df}^{\rm inter} = -0.15$ eV. Even though this is a very rough estimate, it is at least clear that the interatomic term is of the same order of magnitude as the intra-atomic term, but has the opposite sign. Therefore it is possible that the value of $I_{\rm df}$ for d_σ is negative and thus $I_2^{(\circ)}$ in Eq. (24) is positive.

For a numerical estimate, Eq. (24) may be rewritten as

$$|I_2^{(c)}|^2 = \frac{4 U(f, f) |U(p, f)|^2}{U(p, d) |U(f, d)|^2} I_2^{(KA)} I_2^{(df)}.$$
 (26)

The value of the dimensionless factor in this expression is estimated to be 5.2 for EuO and 4.0 for EuSe. This means that for EuSe, even if the ratio $I_2^{(\mathrm{KA})}/I_2^{(\mathrm{df})}$ is only 1/20, $|I_2^{(\mathrm{ef})}|/|I_2^{(\mathrm{df})}|$ is fairly large, about 0.45. For EuO the ratio $I_2^{(\mathrm{KA})}/I_2^{(\mathrm{df})}$ is expected to be substantially larger than that for EuSe since $t(\mathrm{p}_\sigma,\mathrm{f}_\sigma)$ increases much faster than $t(\mathrm{p}_\sigma,\mathrm{d}_\sigma)$, because of the well-localized character of the 4f wave function. Therefore, with the help of the first factor in Eq. (26), $I_2^{(\mathrm{e})}$ may become larger than $I_2^{(\mathrm{df})}$ and thus I_2 of EuO may be positive.

A mechanism similar to our d-f exchange was evaluated by de Graaf and Xavier. ²⁹ They calculated the second-order d-f exchange interaction based on a crude band model and claimed that this interaction is responsible for I_1 , the nn exchange constant. As is clear from the present treatment, however, the mechanism is very sensitive to the band structure and the transition matrix element. Most of the

second-order terms based on molecular orbitals cancel each other in the atomic orbital picture and only the sixth-order terms with respect to the band gap remain. These terms are responsible for I_2 and in this sense de Graaf and Xavier's model and treatment of this mechanism are too crude to predict a reasonable result.³⁰

As was reviewed by Anderson,⁵ there are many other processes that contribute to I_2 . Although they are all estimated to be less important for the case of Eu chalcogenides than the mechanisms already discussed, some of them are mentioned briefly below.

1) The exchange type $f_1 \to f_2$ transfer mechanism is described by the matrix element

$$\langle \mathbf{f}_{\sigma 1}(\mathbf{r}_i) \mathbf{p}_{\sigma 0}(\mathbf{r}_j) | e^2 / r_{ij} | \mathbf{f}_{\sigma 2}(\mathbf{r}_j) \mathbf{p}_{\sigma 0}(\mathbf{r}_i) \rangle.$$
 (27)

This should be compared with Eq. (3), which leads to 0.013 eV as the transfer energy for EuSe. However, due to the small p_{σ} - f_{σ} overlap, the value of (27) is about one order of magnitude smaller than that of (3).

- 2) The excited state in which two p_{σ} electrons with opposite spins are transferred from a given anion to the Eu sites on either side is responsible for I_2 and is described by a fourth-order perturbation term. In this case the energy denominator is larger, without substantial change in the numerator, than those of previously described mechanisms, thus yielding a smaller contribution.
- 3) The direct ferromagnetic p_{σ} - f_{σ} interaction in the sense of Heisenberg contributes to I_2 and is described by a third-order perturbation term. This contribution is usually smaller than or cancels 2).

Indirect exchange mechanisms (I1)

In this category are included the mechanisms in which the cation wave functions have the more important role and the anion p bands are relatively unimportant. Since the overlap among the cation wavefunctions is most significant between nn cations, the principal contribution of this mechanism is to I_1 .

The filled cation wavefunctions are 4f and the closed shells 5s and 5p; therefore the transfer of 4f or 5p electrons to the vacant 5d, 6s or 4f states should be responsible for the mechanism. In the following, these transfers are considered.

Odd parity transfer mechanism

At first we consider the mechanism in which a 4f electron is transferred to a crystal 5d or 6s state. This virtual excited state seems to be important because the activation energy is very small, as is seen in Fig. 1. The transition is observed in optical absorption spectra typically as the first absorption peak, ¹⁰ and is interpreted as a magnetic exciton state extending mostly onto the nn Eu sites. ¹² (This transition is responsible for various anomalous mag-

neto-optical phenomena.) However, both the lowest s and d magnetic excitons are of even parity, different from the odd parity of the f state. Therefore neither of them is excited by the usual even parity perturbation, e.g., the Coulomb interaction. In such a situation the most important perturbation should be due to phonon vibrations, particularly optical phonons, and the zero-point vibration at T=0. Then the following third-order process would be responsible for I_1 : A 4f electron is excited to a magnetic exciton state I, experiences the usual s-f or d-f exchange interaction at the nn Eu site, and returns to the initial state.

For simplicity, we consider only the magnetic exciton formed by the $d\varepsilon$ functions³¹; the extension to other cases is straightforward. The potential due to the lattice vibration is written as

$$(\pi/R_0)^2 D\mathbf{r} \cdot \delta \mathbf{R},\tag{28}$$

in which D is the electron-phonon coupling constant (usually a few eV), R_0 is the nn Eu-chalcogen distance, \mathbf{r} is the vector from the center of the central Eu ion and $\delta \mathbf{R}$ is the relative distortion of the Eu ion. Furthermore, if we introduce the average probability that the magnetic exciton is located on a particular nn Eu site, $\langle \alpha_1^2 \rangle$, and the average excitation energy of the exciton, Δ , the third-order perturbation term for I_1 may be written in terms of the oscillator strength P, which corresponds to photoabsorption to the magnetic exciton state, because there is a similarity between the electron-optical phonon interaction and the electron-photon interaction. Then the exchange constant is written as

$$I_1^{\text{(op)}} = h^2 \langle \alpha_1^2 \rangle I_{\text{df}} D^2 (\pi/R_0)^4 \langle (\delta \mathbf{R})^2 \rangle P / (2mS_f \Delta^3), \quad (29)$$

in which

$$\langle (\delta \mathbf{R})^2 \rangle = 3 \, h (1 + 2N_o) / (2M_r \omega_o) \tag{30}$$

is the average squared fluctuation of the lattice point, m is the electron mass, $M_{\rm r}$ is the reduced anion-cation mass, $\omega_{\rm o}$ is the average optical phonon angular frequency, and $N_{\rm o}$ is the average occupation number of the optical phonon. The oscillator strength is 32

$$P = (2m/3h^2) \sum_{l} \alpha_{0l}^2 \Delta_l |\langle i| \mathbf{r} | f \rangle|^2, \qquad (31)$$

in which \sum_{l} means the summation over all available magnetic exciton states. Equation (29) shows that the sign of $I_{1}^{(op)}$ is the same as that of I_{df} or I_{sf} . Here I_{df} is mostly due to d ϵ states and I_{sf} is mostly due to electrons near the bottom of the 6s band. Therefore, as was discussed previously, the atomic value is applicable and I_{df} and I_{sf} are positive.

For the calculation, the following values are used for EuO³³: $\langle \alpha_1^2 \rangle = 1/12$, $I_{\rm df} = 0.1$ eV, D = 4 eV, $^{34}R_0 = 2.57$ Å, $\hbar\omega_0 = 0.025$ eV, $\Delta = 2.5$ eV and $P = 10^{-2}$.

Most of these values are obviously overestimated; nevertheless the calculated value,

$$I_1^{\text{(op)}} = 3.5 \times 10^{-6} \text{ eV for EuO (at } T = 0),$$
 (32) is much smaller than the experimental value, $4.7 \times 10^{-5} \text{ eV}.$

Smit³⁵ proposed a similar mechanism and declared that it agreed in order of magnitude with the experimental value. In his calculation, however, the pure atomic picture was used instead of the magnetic exciton model. Therefore, fifth-order perturbation theory was necessary and, further, the calculation included various ambiguities. In particular, he used an unusually large electron-phonon coupling con-

stant, which seems to be the largest error. As is seen in Fig. 4, the overlap of 4f and 5d wavefunctions is not large and thus the oscillator strength P is substantially smaller than one. Also, the fluctuation due to the lattice vibration is not large; for example, $\frac{1}{3}\langle(\delta \mathbf{R})^2\rangle_o$ is 5.2×10^{-19} cm² in EuO and 2.5×10^{-19} cm² in EuSe. These factors make $I_s^{(op)}$ small.

The remarkable property of $I_1^{\text{(op)}}$ in this mechanism is its strong temperature dependence due to N_o . A careful measurement of the paramagnetic susceptibility of a single crystal of EuS was made by McGuire³⁶ up to 900°K to check this property. No anomalies were found near the optical phonon frequency, in agreement with the present calculation.

• Even parity transfer mechanism

In the preceding section we considered the transfer of a 4f electron to an even parity magnetic exciton state that has substantial amplitude at the central Eu site and lower energy. Here we consider the transfer to the odd parity magnetic exciton state. This type of excitation has the disadvantage that the average energy is higher and, since there is no amplitude of the atomic d or s orbital at the central Eu, the transfer matrix is essentially due to the interatomic overlap. The advantage of this mechanism over the previous one is that now the usual even parity perturbation is available, which is much larger than the odd parity perturbation due to the electron-phonon interaction. Here again for simplicity we consider only 5d orbitals.

In the cubic crystal environment, the 4f wave functions are separated into three groups. Among them the t_{2u} group with triple degeneracy has the largest overlap between nn Eu sites. ³⁷ For the 5d states on the nn Eu sites, d ϵ , the angular dependence (xy, yz and zx) causes the largest overlap with $t_{2u}(4f)$. Then the third-order perturbation, similar to that of the preceding section but due to the usual transfer energy, gives the exchange constant

$$I_{1}^{(ep)} = (I_{df}/S_{f}) \sum_{l} \alpha_{l1}^{2} |t(t_{2u}, l)|^{2} / U_{l}^{2}$$

$$= 2I_{df} |t(t_{2u}, d\epsilon)|^{2} / S_{f} U^{2}, \qquad (33)$$

in which \sum_l means the summation on all the possible t_{2u} type magnetic excitons and α_{l1}^2 is the probability for the lth magnetic exciton to be located on a particular Eu site. This mechanism may be described as follows. By the transfer effect, the real t_{2u} wave function is a mixture of the $t_{2u}(4f)$ and $t_{2u}(d\epsilon)$ functions. The tail part of the t_{2u} function, which is the $t_{2u}(d\epsilon)$ function, gives the direct intra-atomic exchange interaction with the 4f spins on the nn Eu site through the d-f exchange interaction. Since the $d\epsilon$ function is responsible for the exchange integral I_{df} , this latter quantity should be positive and thus $I_1^{(ep)}$ should also be positive.

For the numerical calculation for EuO, we use $I_{\rm df} = 0.1$ eV and U = 4 eV. The main problem is estimation of the transfer energy between the $t_{\rm 2u}(4f)$ function and the corresponding $d\epsilon$ function, $t(t_{\rm 2u}, d\epsilon)$. As may be seen in Fig. 4, the overlap³⁸ between f_{σ} and d_{σ} states in EuO is similar to that between f_{σ} and p_{σ} states. A preliminary calculation shows that the former is about one-third the value of the latter. Therefore, considering the difference in the angular dependences, we may put

$$t(t_{2n}, d\epsilon) \approx 0.1 \text{ eV},$$
 (34)

compared with $t(f_{\sigma}, p_{\sigma}) = 0.45$ eV. Then we get

$$I_1^{(ep)} \approx 3.5 \times 10^{-5} \text{ eV},$$
 (35)

which is in good agreement with the experimental value, 4.6×10^{-5} eV. This mechanism is consistent with the empirical result that I_1 decreases very rapidly with increasing lattice constant, as shown in Fig. 3, because $t(t_{2u}, d\epsilon)$ decreases rapidly with increasing Eu-Eu distance, as may be seen in Fig. 4. That I_1 depends more on the nn Eu distance than on the character of the anion is clearly demonstrated by high pressure experiments in which the $\Delta\theta$ -vs- ΔR_0 data fall on the θ curve of Fig. 3. It is also interesting to note that the R dependence of the overlap integral for rather small overlap is approximately R^{-4} , but that for a wider range the dependence is $\exp(-4R/R_0)^{21}$. Assuming that $I_1^{(ep)}$ is proportional to the square of the overlap between the t_{2u} and $d\epsilon$ functions, we have the relation

$$I_1^{\text{(ep)}}(R) = I_1^{\text{(ep)}}(R_0) \exp(-8R/R_0),$$
 (36)

in which $I_1^{(ep)}(R_0)$ is the value for EuO and R_0 is the nn Eu distance in EuO. The prediction of Eq. (36) fits the experimental line for I_1 in Fig. 3 very well. For example, the ratio of I_1 for EuO and for EuSe is 5.2 according to Eq. (36) and 4 in the experiment. The present mechanism also contributes to the crystal field splitting of a 4f state because the energy of the t_{2u} state is suppressed by the amount

$$-8|t(t_{2u}, d\epsilon)|^2/U(f, d) = -0.045 \text{ eV for EuO.}$$
 (37)

There are many other processes that belong in the present category and are available to contribute to I_1 . Two of them are mentioned briefly.

1) The process in which a 4f electron at site n is transferred to a d ϵ state at site m, then a 4f electron at site m is transferred to a d ϵ state at site n, and finally both return to the initial state through the exchange-type Coulomb interaction,

$$\langle 4f_n(1), 4f_m(2)|e^2/r_{12}|d\epsilon_n(2), d\epsilon_m(1)\rangle,$$
 (38)

is a third-order process and is smaller than the principal process of this section due to the small overlap between $d\epsilon_n$ and $4f_m$ functions.

2) The lowest-order perturbation is the second-order process with respect to the matrix element of (38), but the resulting contribution to I_1 is still smaller than the principal one because it includes the fourth power of the d ϵ -4f interatomic overlap integral as a factor.

Finally, it may be worthwhile to repeat the comment that the polarization effects of the 5s and 5p states have not been treated explicitly so far, but these may have been included implicitly in the effective transfer energies for the 4f states.

The following comments were generated by questions asked after the oral presentation of this paper.

- 1) The convergence of the perturbation calculations is good because the expansion parameter t(l, l')/U(l, l') is small, about 10^{-1} to 10^{-2} .
- 2) The author's opinion, as evidenced in this paper, is that it is more reliable to estimate t(l, l') empirically from experimental data than to attempt a first-principles calculation.
- 3) An example of a ferromagnetic coupling constant I_2 for the 180-degree configuration may be EuTiO₃ [see T. R. McGuire, M. W. Shafer and R. J. Joenk, *J. Appl. Phys.* 37, 981 (1966)].

Acknowledgments

The author expresses his thanks to T. R. McGuire for his careful measurement of the paramagnetic Curie point of EuS; to D. T. Teaney, V. L. Moruzzi, E. L. Boyd and G. Burns for discussions of their unpublished data; and to S. Methfessel, S. von Molnar and P. E. Seiden for interesting discussions and their kind hospitality during his stay at the IBM Research Center. Valuable discussions with A. Yanase are also greatly appreciated.

References and notes

 See, for example, the review paper by C. Herring in Magnetism, edited by G. T. Rado and H. Suhl, Vol. IV, Academic Press, Inc., New York 1965, p. 1.

- C. Zener, Phys. Rev. 81, 440 (1951); ibid. 82, 403 (1951); ibid. 83, 299 (1951).
- 3. T. Kasuya, Progr. Theoret. Phys. (Kyoto) 16, 45 (1956); ibid. 16, 58 (1956).
- For example, T. Kasuya, Magnetism, edited by G. T. Rado and H. Suhl, Vol. IIB, Academic Press, Inc., New York 1966, p. 215.
- For a review, P. W. Anderson, Magnetism, edited by G. T. Rado and H. Suhl, Vol. I, Academic Press, Inc., New York 1963, p. 25, or Solid State Physics, edited by F. Seitz and D. Turnbull, Vol. 14, Academic Press, Inc., New York 1963, p. 99.
- For example, J. B. Goodenough, J. Phys. Chem. Solids 6, 287 (1958) or J. Kanamori, J. Phys. Chem. Solids 10, 87 (1959).
- For example, the series of discussions on KNiF₃ S. Sugano and R. G. Shulman, *Phys. Rev.* 130, 517 (1963);
 R. E. Watson and A. J. Freeman, *Phys. Rev.* 134, A1526 (1964);
 S. Sugano and Y. Tanabe, *J. Phys. Soc. Japan*, 20, 1155 (1965).
- R. E. Watson and A. J. Freeman, *Phys. Rev.* 133, A1571 (1964); ibid. 139, A1606 (1965); ibid. 156, 251 (1967).
- For the atomic wave functions of rare earth metals consult A. J. Freeman and R. E. Watson, Phys. Rev. 127, 2058 (1962); F. Herman and S. Skillman, Atomic Structure Calculations, Prentice-Hall, Inc., New York 1963; A. J. Freeman, J. O. Dimmock and R. E. Watson, Quantum Theory of Atoms, Molecules, and the Solid State, edited by P. O. Löwdin, Academic Press, Inc., New York 1966, p. 361; J. T. Waber and D. T. Cromer, J. Chem. Phys. 42, 4116 (1965). The differences among the values presented are very small.
- For reviews, T. Kasuya and A. Yanase, Rev. Mod. Phys.
 40, 684 (1968); S. Methfessel and D. C. Mattis, Handbuch der Physik, edited by S. Flügge, Vol. XVIII/1, Springer-Verlag, Berlin 1968, p. 389.
- 11. T. Kasuya, J. Appl. Phys. 41, 1090 (1970).
- A. Yanase and T. Kasuya, J. Phys. Soc. Japan 25, 1025 (1968); also Ref. 10.
- 13. S. J. Cho, Phys. Rev. 157, 632 (1967).
- 14. See Ref. 10 for a detailed discussion.
- 15. For an example of the band structure of the transition metals see B. Segall, *Phys. Rev.* 125, 32 (1962).
- T. R. McGuire, B. E. Argyle, M. W. Shafer and J. S. Smart, J. Appl. Phys. 34, 1345 (1963); T. R. McGuire and M. W. Shafer, J. Appl. Phys. 35, 984 (1964); G. Busch, B. Natterer and H. R. Neukomm, Phys. Letters 23, 190 (1966). The values in Fig. 3 are somewhat different from those of the above references because the former values have been corrected using specific heat and NMR data, etc. (see Ref. 10).
- J. D. Axe and G. Burns, Phys. Rev. 152, 331 (1966);
 G. Burns and J. D. Axe, Optical Properties of Ions in Crystals, edited by H. M. Crosswhite and H. W. Moos, Interscience Publishers, New York 1967, p. 53.
- R. E. Watson and A. J. Freeman, Phys. Rev. 156, 251 (1967).
- 19. There are no definite experiments concerning the crystal field due to the covalent bonding in rare earth compounds in which this mechanism is apparently predominant over that of the static crystal field. Generally, the energy associated with this mechanism is expected to be about 0.05 to 0.1 eV in most compounds. See, for example, Refs. 17 and 18 and the references in those papers; also see J. M. Baker, W. B. J. Blake and G. M. Copland, *Proc. Roy. Soc. (London)* A309, 119 (1969).

- 20. The situation depends, of course, on the material. If the $p \rightarrow s$ transfer is much larger than the $p \rightarrow d$ transfer, or if I_{at} becomes smaller due to cancellation, the s state will be more important.
- For example, Ref. 7; also G. Burns and J. D. Axe, J. Chem. Phys. 45, 4362 (1966).
- 22. Since the 5d wave functions are fairly extensive spatially, their overlap with p_{π} functions is not small; see, for example, Ref. 17.
- See the reviews in Ref. 10; numerous references are cited therein. Also see W. J. Scouler, J. Feinleib, J. O. Dimmock, T. B. Reed and C. R. Pidgeon, J. Appl. Phys. 41, 1085 (1970) and C. R. Pidgeon, J. Feinleib, W. J. Scouler, J. O. Dimmock and T. B. Reed, IBM J. Res. Develop. 14, 309 (1970).
- 24. The actual band is an s-d admixture and both the s-p_{\sigma} and d_{\sigma}-p_{\sigma} transfer energies are concerned. This effect may be canceled partly or overwhelmingly by d-p_{\sigma} transfer energies, which are neglected here.
- 25. See Ref. 10 for a treatment of the hopping activation energy due to the s-f exchange interaction, and also the discussion of the Appendix therein. The resistivity of a fairly well-doped sample also indicates that I_{st} is about 0.03 to 0.04 eV; see S. von Molnar and T. Kasuya, *Phys. Rev. Letters* 21, 1757 (1968).
- See p. 286 of Ref. 4; also see R. E. Watson, S. Koide, M. Peter and A. J. Freeman, *Phys. Rev.* 139, A167 (1967).
- 27. The mechanism underlying the negative exchange energy is described by P. W. Anderson, *Phys. Rev.* 124, 41 (1961).
- 28. J. Kondo, Progr. Theoret. Phys. (Kyoto) 32, 37 (1964).
- A. M. de Graaf and R. M. Xavier, *Phys. Letters* 18, 225 (1965); R. M. Xavier, *Phys. Letters* 25A, 226 (1967).

- 30. For example, de Graaf and Xavier claim that the k dependence of the valence p bands may be omitted. However, it is clear that, in such a case with a constant matrix element, the resultant exchange constant is zero.
- 31. The first absorption peak is believed to be due to the dε state; see Ref. 10.
- 32. For example, M. J. Freiser, S. Methfessel and F. Holtzberg, J. Appl. Phys. 39, 900 (1968). Note that a factor 1/3 is missing from Eq. (2) of this paper.
- 33. For EuF₂ see Ref. 32; the details for Eu chalcogenides are presently in unpublished work by the author.
- See Ref. 25; also see S. von Molnar and M. W. Shafer,
 J. Appl. Phys. 41, 1093 (1970).
- 35. J. Smit, J. Appl. Phys. 37, 1455 (1966).
- 36. T. R. McGuire, private communication.
- 37. The wave functions have the following symmetries: $z(x^2 y^2)$, $x(y^2 z^2)$ and $y(z^2 x^2)$.
- 38. Note that in this case the principal direction is that joining the nearest neighbor Eu sites.
- R. Stevenson and M. C. Robinson, Can. J. Phys. 43, 1744 (1965); G. K. Sokolov, K. M. Demchuk, K. P. Rodionov and A. A. Samokhvalov, Soviet Phys.-JETP, 49, 317 (1966); P. Schwob and O. Vogt, Phys. Letters 24A, 242 (1967); G. Busch, P. Schwob and O. Vogt, Phys. Letters 20, 602 (1966). There are considerable deviations among the data of the above papers, due mostly to ambiguity in the compressibility results. However, the average tendency fits well with the θ curve in Fig. 3.

Received November 10, 1969